Effect of conductive additives to gel electrolytes on activated carbon-based supercapacitors

Farshad Barzegar,[1] Julien K. Dangbegnon,[1] Abdulhakeem Bello,[1] Damilola Y. Momodu,[1] A. T. Charlie Johnson, Jr.,[2] and Ncholu Manyala[1,a]
[1]*Department of Physics, Institute of Applied Materials, SARCHI Chair in Carbon Technology and Materials, University of Pretoria, Pretoria 0028, South Africa*
[2]*Department of Physics and Astronomy, University of Pennsylvania, Philadelphia, PA 19104, USA*

(Received 19 June 2015; accepted 16 September 2015; published online 24 September 2015)

This article is focused on polymer based gel electrolyte due to the fact that polymers are cheap and can be used to achieve extended potential window for improved energy density of the supercapacitor devices when compared to aqueous electrolytes. Electrochemical characterization of a symmetric supercapacitor devices based on activated carbon in different polyvinyl alcohol (PVA) based gel electrolytes was carried out. The device exhibited a maximum energy density of 24 Wh kg^{-1} when carbon black was added to the gel electrolyte as conductive additive. The good energy density was correlated with the improved conductivity of the electrolyte medium which is favorable for fast ion transport in this relatively viscous environment. Most importantly, the device remained stable with no capacitance lost after 10,000 cycles. [http://dx.doi.org/10.1063/1.4931956]

INTRODUCTION

There has been a tremendous increase on sustainable storage technology due to rapid depletion of current sources of energy (fossil fuel). Supercapacitors, batteries and fuel cells are all under investigation for sustainable energy technologies such as energy generation, energy conversion and energy storage. Electric double-layer capacitors (EDLCs), also known as ultracapacitors or supercapacitors, are high power density devices with long cycle life and are considered as a leading candidate for zero CO_2 emission vehicles by providing peak power for start-stop, acceleration and regenerative braking systems.[1,2]

EDLCs store energy by accumulation of charge at the interface between the electrode and electrolyte. The material of choice for most common and commercially available EDLCs is carbon due to its fair conductivity and high surface area ranging from 500 $m^2\ g^{-1}$ to 3000 $m^2\ g^{-1}$.[3] Current research activities focus on trying to increase the energy density of EDLCs without sacrificing their intrinsic high power density and long cycle life as well as minimizing fabrication cost by using abundant sources of carbon which are also environmentally friendly. One approach to achieve this is the use of electrolyte with a large potential window since the energy density of EDLCs is a function of the voltage squared ($E = 0.5CV^2$)[4] while the voltage range is limited or governed by the type of electrolyte used.

Recently three dimensional porous carbons have become attractive as materials for EDLCs because of their texture, structural composition, and high density of micropores. It has been shown that the pore size distribution of the material influences the electrochemical performance of the electrode material in various electrolytes.[5] The size distribution can be classified into macro-, meso- and micropores, while the electrolytes are categorized as ionic liquids, and organic and aqueous electrolytes. These different electrolytes have different advantages and disadvantages. Aqueous

[a]Corresponding author: N. Manyala (Ncholu.Manyala@up.ac.za)

electrolytes are characterized by high conductivity and high mobility of proton transport but suffer from low potential range (limited to ~1.2 V due to water decomposition) in power sources and are also associated with leakage resistance and corrosion.[6] On the other hand, organic and ionic liquids allow EDLCS to operate between 2.3 and 4 V in different solvents leading in principle to high energy density,[7] but suffer from low conductivity, high viscosity which slows ion transport and hence high resistance of the EDLCS, which can lead to low power density.

For application of supercapacitors in mobile communication and computing electronics, a key component is the solid-state electrolyte.[8] Solid state polymer-based gel electrolytes, comprising of a polymer and an ionic component, have recently been explored because of their anticorrosive properties, making them compatible with metal current collectors which exhibit good physical contact and good ionic conductivity with high stability over cycling, simple principle and mode of fabrication which are more reliable, environmentally friendly and safe to handle.[9–12] They are also characterized by wider electro-chemical potential window (> 4 V).[13,14] Polymer gel based electrolytes have been used in electrochemical supercapacitors applications, for example polyvinyl alcohol (PVA)–KOH,[15] PVA–H_2SO_4[16] and PVA-H_3PO_4.[17] Recently, Ma *et al*. reported a redox-mediated P-phenylenediamine doped polyvinyl alcohol gel electrolyte (PVA-KOH-PPD) as electrolyte and separator, and activated carbon as electrodes for symmetric supercapacitor with excellent electrochemical performance.[18] The same activated carbon electrode was tested in PVA-KOH-$K_3[Fe(CN)_6]$ gel electrolyte by the same authors and the material showed a specific capacitance as high as 431 F g^{-1}, energy and power densities values of 57.94 Wh kg^{-1} and 59.84 kW kg^{-1}, respectively.[19] The excellent good electrochemical performance was attributed to high ionic conductivity of gel electrolyte and the contribution from the reversible redox reaction of $K_3[Fe(CN)_6]$ and its quick electron relay at the electrode-electrolyte interface.[19] Ramasamy *et al*. reported activated carbon supercapacitor using a gel electrolyte of sodium salt-polyethylene oxide in an organic mixture solvent with the cell operating at a stable potential window of 2.5 V and exhibiting a specific capacitance of 24 F g^{-1}, real power of 0.52 kW kg^{-1}, and energy density of 18.7 Wh kg^{-1}. Gao *et al*. also tested an asymmetric capacitor via paper-like carbon nanotube-manganese oxide electrodes based on potassium polyacrylate gel-based with a cell voltage of 1.8 V, a stable cycling performance (capacitance retention of 86.0 % after 10,000 continuous charge/discharge cycles) and energy of density (32.7 Wh kg^{-1}).[20] Here we report on the electrochemical performance of the symmetric supercapacitors based on highly porous activated carbon material and solid-state poly-vinyl alcohol (PVA) and potassium hydroxide (KOH) hydrogel electrolyte with different additives such as carbon black (CB) and a conducting polymer Polyaniline (PANI). A comparative electrochemical study with four different electrolytes in terms of their specific capacitance, energy and power density was performed. The gel polymer electrolytes obtained at the different dopants were denoted as PK, PKC, and PKP for PVA-KOH, PVA-KOH-CB and PVA-KOH-PANI hydrogels respectively. The PKC sample exhibited a maximum energy density of 24 Wh kg^{-1} with no capacitance loss after 10,000 galvanostatic charge/discharge cycles.

EXPERIMENTAL

Preparation of gel polymer electrolytes

The gel polymer electrolytes were prepared by a modification of the procedure in Ref. 18. First, 5 ml PVA 10 wt% and 5 ml KOH 6 M were mixed by continuous stirring at 85 °C until homogeneous viscous mixture was obtained and allowed to cool to room temperature. This mixture of PVA–KOH gel polymer was designated as **PK**. To this PVA-KOH electrolyte, 5 mg carbon black was added to obtain PVA-KOH-carbon black electrolyte denoted as **PKC**, and 5 mg polyaniline was added to another mixture of **PK** to obtain PVA-KOH- polyaniline denoted as **PKP** respectively.

Preparation of activated carbon electrode

The AC used in this work was prepared as follows; graphene foam (GF) was first prepared by chemical vapour deposition (CVD) onto a catalytic nickel foam (Alantum Innovations in Alloy

Foam Munich, Germany) following the procedure described in our previous report.[21] To provide mechanical support for the graphene during removal of nickel, polymethylmethacrylate (PMMA) was drop coated on the sample and baked at 180 °C for 30 minutes. The samples were then placed in 3 M HCl solution at 80 °C overnight to ensure that nickel was completely etched away. The resulting GF sample was placed in acetone at 50 °C for 30 minutes to remove the PMMA. The samples were then rinsed in deionised water and dried.[22]

The hydrogel was synthesised via the hydrothermal process. Typically, 100 mg of GF were dispersed in 100 ml of water containing 11.11 g of polyvinyl alcohol (PVA) followed by the addition of different masses of 1.76 g Polyvinylpyrrolidone (PVP) in a glass vial by ultrasonication, 1.50 ml of hydrochloric acid (HCl) was added to the solution as a cross linker. The mixture was sonicated for few minutes and further stirred for 30 min to obtain a homogeneous dispersion before being transferred into a 120 ml Teflon-lined autoclave system operated at 190 °C for 12 h. The resulting hydrogel was crushed and washed with deionized water and dried for 6 h. The hydrogel obtained was then soaked in aqueous KOH solution with a KOH/hydrogel mass ratio of 5 for 24 h and dried at 120 °C for 12 h before carbonization. The composite was then placed in a horizontal tube furnace ramped from room temperature to 800 °C at 10 °C/min under argon gas flow for 1 h of activation. This procedure transforms the hydrogel into carbon materials consisting of a continuous pore network distribution. After which sample was washed with 3 M HCl to remove the remaining KOH and further washed with deionized water and dried in an electric oven. To prepare the electrode, the AC and binder polyvinylidene fluoride (PVDF) were homogeneously mixed in an agate mortar with respective weight ratio 90:10 at room temperature and dispersed in N-methylpyrrolidone (NMP) solution to form slurry. The slurry was then uniformly coated on a nickel foam current collector and dried at 60 °C in an oven for 8 hours to ensure complete evaporation of the NMP.

Supercapacitor assembly

A symmetric supercapacitor was fabricated by dropping the hydrogel electrolyte between the AC electrodes and filter paper separator as shown in scheme 1 below.

Characterization

Nitrogen adsorption–desorption isotherms were measured at −196 °C using a Micromeritics ASAP 2020 analyzer. All the samples were degassed at 180 °C for more than 12 h under high vacuum conditions. The surface area was calculated by the Brunauer–Emmett–Teller (BET) method from the adsorption branch in the relative pressure range (P/P_0) of 0.01 – 0.2. The sample was also characterized using powder X-ray diffraction (XRD). An XPERT-PRO diffractometer (PANalytical

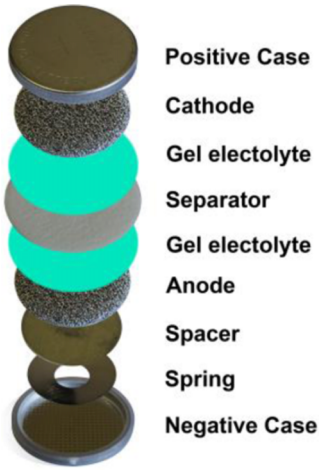

SCHEME 1. Assembly of supercapacitor device.

BV, Netherlands) with theta/theta geometry, operating a cobalt tube at 35 kV and 50 mA was used. The SEM images were obtained on a Zeiss Ultra Plus 55 field emission scanning electron microscope (FE-SEM) operated at an accelerating voltage of 2.0 kV. Transmission electron microscopy (TEM) was carried out with a JEOL JEM-2100F microscope operated at 200 kV accelerating voltage. The electrochemical test of the symmetric cell was carried out in a two-electrode cell configuration by means of coin-type cells with a mass loading of ~3.3 mg for both electrodes, a thickness of 0.2 mm and a diameter of 16 mm, using a glass microfiber filter paper as the separator, in KOH and three different hydrogel electrolytes respectively. All electrochemical measurements were carried out using a Bio-logic VMP-300 potentiostat. These measurements included cyclic voltammetry (CV), chronopotentiometry (CP) and electrochemical impedance spectroscopy (EIS). The CV tests were carried out at different scan rates ranging from 5 to 100 mV s^{-1}, and the electrochemical impedance spectroscopy (EIS) measurements were conducted in the frequency range from 0.1 to 100 kHz with an open circuit potential (~ 0 V).

RESULTS AND DISCUSSIONS

Figure 1 shows SEM images for the structural characterization of the activated carbon used in this work. Figure 1(a) and 1(b) show the low and high magnification micrograph of the activated carbon. Highly porous network are observed which could be beneficial in providing easy ion mobility for fast ion transport for high-performance supercapacitors. To study the crystallinity of the carbon material, XRD was performed and the spectrum is shown in figure 2(a). All the XRD peaks are identified as graphite peaks (COD: 96-900-8570) which crystallizes in the orthorhombic structure with space group P63mc(186), lattice parameters a = 2.4560 Å and c = 6.6960 Å. Figure 2(b) shows the N_2 gas sorption analysis of the sample showing a H4 adsorption and desorption hysteresis, characteristic of complex materials containing both micropores and mesopores. The sample exhibits a high BET surface area of 2994 m^2 g^{-1} and an average Barrett-Joyner-Halenda (BJH) pore size (inset to Figure 2(b)) centered at about 8 nm depicting substantial amount of mesopores. The sharp increase of the curve for diameter below 2 nm also hints the presence of micropores in this sample. The presence of micropores and mesopores in this sample are highly desirable for energy storage application since micropores store the charges whereas mesopores allow ion accessibility to the micropores. Also from the SEM micrographs, macropores are also observed which could act as buffer.

Electrochemical characterization

Cyclic voltammetry measurements of the activated carbon were performed with the different polymer gel electrolytes in a two electrode configuration and the results obtained were compared with results obtained using KOH aqueous electrolyte alone. Figure 3 shows the different CV curves obtained in different polymer gel electrolytes at the scan rate of 10 mV s^{-1}. The CV curves of the activated carbon in the aqueous electrolyte operate up to a potential window of 1.6 V while

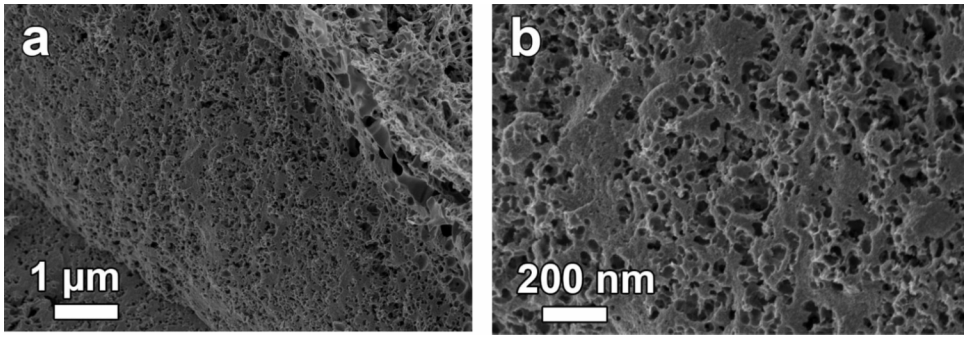

FIG. 1. (a) and (b) low magnification and high magnification SEM images of AC respectively.

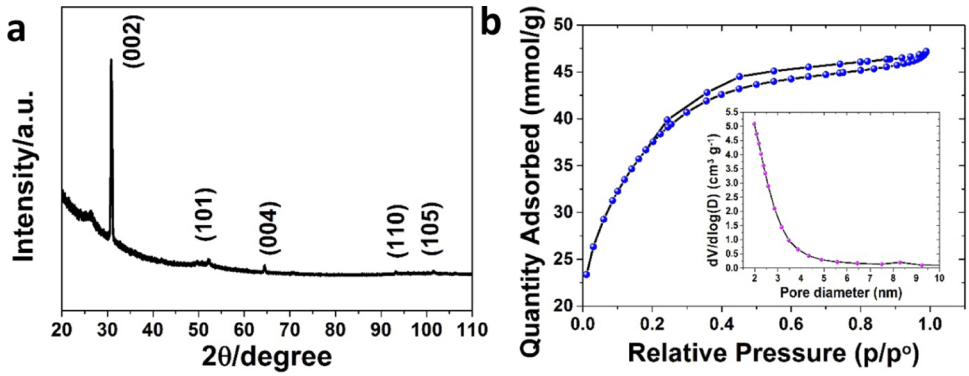

FIG. 2. (a) X-ray diffraction and (b) the N_2 adsorption-desorption isotherm of the AC.

those in the gel electrolytes operate up to a potential window of 2.0 V. Furthermore, these results show that the CV curves for all these cells show fairly rectangular shape, indicating EDLC behavior with good capacitive behavior with rapid current responses. Moreover, a clear increase in current response is observed from aqueous to gel electrolytes. Furthermore, the devices using PK and PKP electrolytes show current leap at a potential of ~1.9 V and towards the 0 V mark, which is attributed to the evolution of gases or oxygenated surface functionalities generated from the electrode and the reactions with the electrolyte during the scanning process. Compared with other two polymer gel electrolytes, devices made with the PKC electrolyte showed a stable and rectangular shape during scanning, which is an indication of pure electrochemical double layer behavior.

Galvanostatic charge-discharge measurements were also performed to evaluate the electrochemical performance of activated carbon in a symmetric capacitor using different polymer gel electrolytes media. At a current density of 1 A g^{-1}, all the cells show symmetric triangular charge/discharge features, which are characteristic of ideal capacitor behavior (Figure 4(a)). The gravimetric capacitance of the devices was calculated from these curves using the expression $C_{SP} = 2I/((dV/dt)m)$, where I is the current (A), dV/dt is the slope of the discharge curve (V) and m is the mass of carbon in one electrode (g). Figure 4(b) shows the specific capacitance as a function of the current density of the symmetric devices. The device with KOH electrolyte showed the highest gravimetric capacitance of 188 F g^{-1} at a current density of 0.5 A g^{-1}, which can be ascribed to the small size of ion in the electrolyte as well as the low viscosity of the electrolyte which enhances a rapid transport mechanism at the interface between the electrode and electrolyte

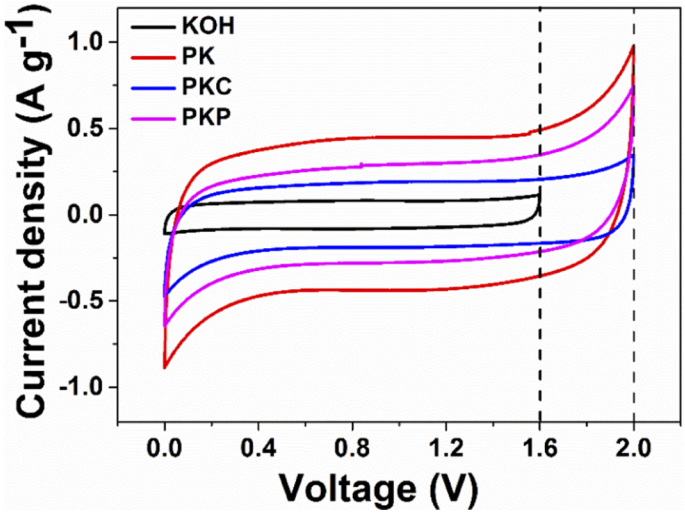

FIG. 3. The CV curves of the supercapacitors in various electrolytes at 10 mV s^{-1}.

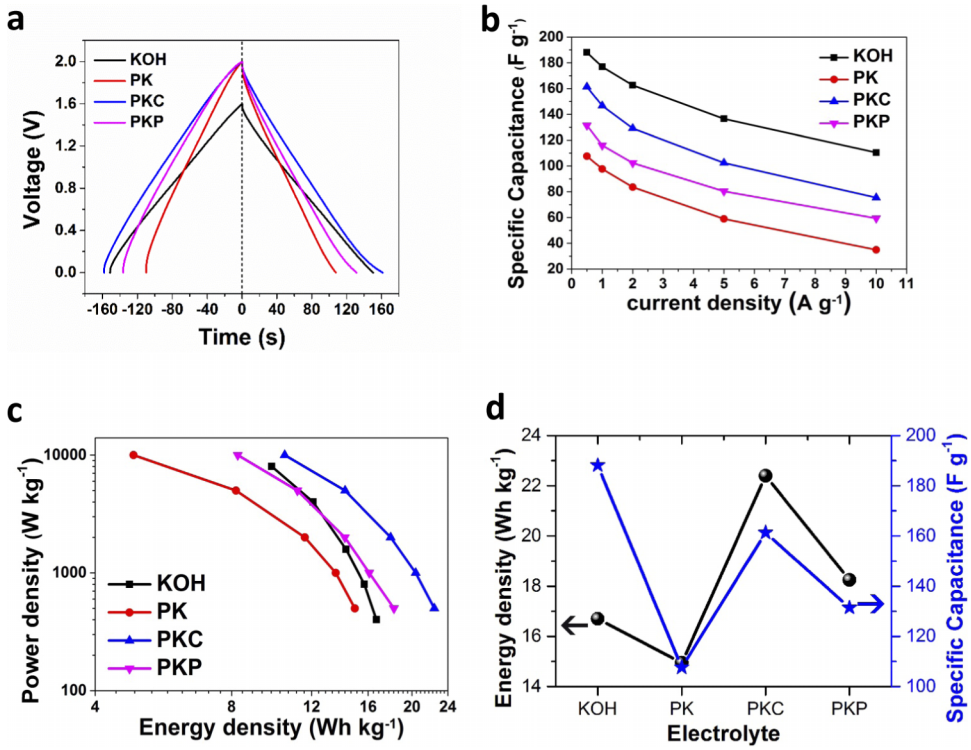

FIG. 4. The comparison of electrolytes dependence of (a) the galvanostatic charge/discharge curves at 0.5 A g^{-1} (b) specific capacitance vs. current density (c) Ragone plot and (d) energy density and specific capacitance vs. electrolytes used in the devices fabricated.

for improved electrochemical performance. Comparing the gel electrolyte-based devices, the device with the PKC performed the best, which could be due to the addition of the carbon black which improves the conductivity of the PVA-KOH gel and hence high capacitance value. The lower values of specific capacitances when the gel electrolytes were used compared to the aqueous electrolyte, could be due to the increase in solution viscosity in the gel electrolyte which reduces the ion conductivity and consequently the ability to accommodate ions in the micropore volume of the electrodes. Although no electrical conductivity measurements were done in this work, carbon black is believed to be a more conducting additive than PANI which was both used as additives in the PK electrolyte as shown by low equivalent series resistance (R_S) that will be discussed below. This is also supported by the higher specific capacitance obtained from the PKC electrolyte in comparison to that obtained in PKP. These specific capacitance values are reasonable for activated carbon as double-layer capacitor and compare favorably to previous values in the literature.[20,23] In order to discard the possibility of the contribution of carbon black and PANI in the total specific capacitance when PKC and PKP electrolytes were used, carbon black and PANI were prepared as electrode material on the nickel foam and the galvanostatic charge- discharge measurements were performed in PVA-KOH electrolyte. This setting will indeed give the contribution of carbon black and PANI in PVA-KOH-CB and PVA-KOH-PANI electrolytes respectively. Figure S1 in the supporting information[25] shows very small discharge time for both materials compared to AC with similar mass of AC as electrode materials. This implies a very little or negligible contribution of these materials in the specific capacitance in PKC and PKP electrolytes, but rather improve the conductivity of the PK electrolyte as stated above.

The Ragone plot of all the devices is shown in figure 4(c) which shows that the lowest value of the energy density was obtained for the PVA-KOH (PK) electrolyte (16 Wh kg^{-1}) which is the electrolyte with the lowest conductivity based on the obtained results. Furthermore, it confirms that the device with the PKC electrolyte has the highest energy density of 24 Wh kg^{-1} which is higher than the value in PKP electrolyte (18 Wh kg^{-1}) at 0.5 A g^{-1}. The energy density values from

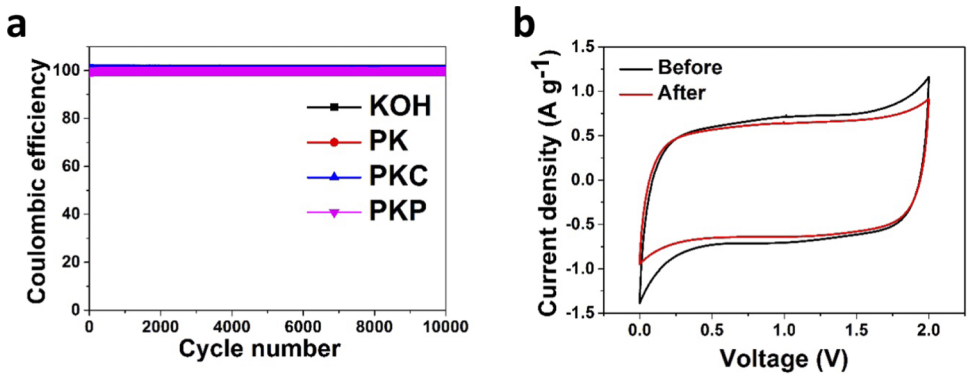

FIG. 5. (a) Cycle stability of different electrolytes at a constant current density of 5 A g^{-1} and (b) CV curves of AC in PKC electrolyte at scan rate of 20 mV s^{-1} before and after cycling.

PKC and PKP electrolytes are due to the extended potential window up to 2.0 V combined with the improved conductivity of the electrolyte medium which also impacts on specific capacitance. This leads to an increase in the energy density and overall performance of the device. This is also evidenced in Figure 4(d) where the energy density and specific capacitance are plotted against the different electrolytes. It is observed that although KOH gives the best specific capacitance, the low voltage window negatively influences the energy density whereas for the PKC electrolyte, a specific capacitance close to that of KOH was obtained with a larger working voltage window which leads to the highest energy density.

Figure 5(a) show the cycle stability of the cell in the different electrolytes at a constant current density of 5 A g^{-1}. The stability of the active material in all electrolytes shows no capacitance loss after 10,000 cycles. The CV curves of PKC at scan rate of 20 mV s^{-1} before and after cycling are shown in Figure 5(b). The Similar CV curves were obtained before and after the 10,000th cycle with better rectangular shape after cycling, implying better EDLC performance after cycling which could be attributed to the fact that during cycling more surface area get exposed to the electrolyte, hence increase in the electrochemical behavior.

Electrochemical impedance spectroscopy (EIS) measurements were performed in the frequency range from 100 kHz to 10 MHz for capacitors operating in the different cells but show similar tendencies as observed in figure 6. The Nyquist plot shown in Fig. 6(a) presents a typical capacitive shape with partial semi-circle in the high-frequency region and vertical line in the low frequency region.

The KOH electrolyte showed a more vertical behavior when compared with gel electrolytes presented in the figure due to its higher conductivity thus demonstrating a better electrochemical diffusion mechanism. At high frequency, the intercept on the real axis (Z′) gives information about the Ohmic resistance (R_s) also known as equivalent series resistance (ESR) of the device. This

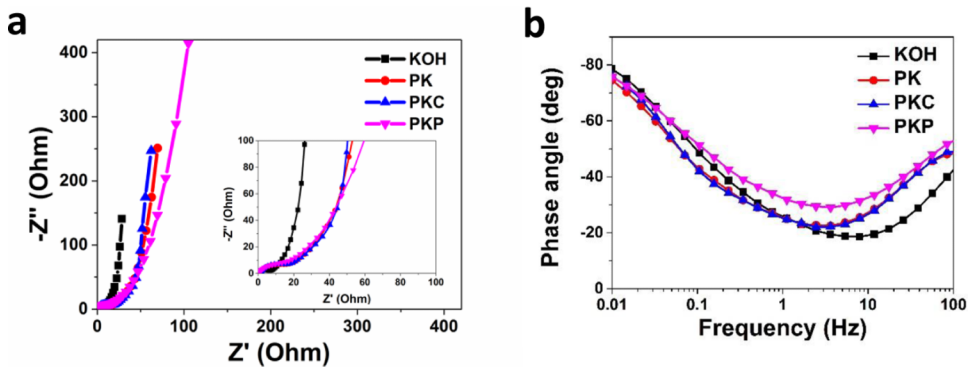

FIG. 6. (a) The Nyquist plots and (b) Bode phase angle plots of AC in different electrolytes.

resistance value includes the intrinsic resistances of the active electrode materials, the substrate and electrolyte, and the contact resistance of the electrodes with the external circuit.[24] From the Nyquist plot above the device with the KOH electrolyte has R_s value of 0.29 Ω. This small R_s value proves that the current can easily diffuse through the electrode-electrolyte interface due to the high mobility of K^+ cation. The three devices made with the gel electrolytes have R_S values of 0.47 Ω, 0.52 Ω and 0.53 Ω for PKC, PK and PKP respectively. The device with the PKC gel electrolyte has a relatively smaller value than the other two gel electrolytes. This difference in R_s can be attributed to the presence of the carbon black in the electrolyte which improves on the conductivity of the gel electrolyte PK much better than PANI. However, comparing with the R_s value from the KOH electrolyte the PKC value is higher. This demonstrates the superiority of aqueous electrolyte over organic and ionic liquid electrolyte which exhibit low conductivity. Fig. 6(b) shows Bode plot for all devices in different electrolytes. It is observed that the cell using KOH aqueous electrolyte shows a phase angle approximately −80° close to −90° for ideal capacitive behavior while the others cells using other three gel electrolytes show a phase angle of ∼78°, which also evidences the good capacitive property of the fabricated supercapacitor cells in these gel electrolytes.

CONCLUSION

The work has demonstrated a simple way to improve the energy density of EDLCs material through using correct electrolyte. The use of conductive additives such as carbon black additive in particular in the gel electrolyte, improved the energy density of the supercapacitor when compared to aqueous electrolyte or simple gel electrolyte. This was correlated with the improved conductivity of the electrolyte medium which is favorable to fast ion transport in this relatively viscous environment. In particular, in this work a maximum energy density of 24 Wh kg^{-1} was obtained when carbon black was added to the gel electrolyte as conductive additive. This value is higher than that obtained in KOH (17 Wh kg^{-1}) and other gel electrolytes PVA-KOH (16 Wh kg^{-1}). Most importantly the cell remained stable with no capacitance loss after 10000 cycles for all devices with PKC device showing slightly higher stability value throughout.

ACKNOWLEDGEMENTS

This work is based on research supported by the South African Research Chair Initiative (SARChi) in Carbon Technology and Materials of the Department of Science and Technology (DST) and the National Research Foundation (NRF). Any opinion, findings and conclusions or recommendations expressed in this work are those of authors and therefore the NRF and the DST do not accept any liability with regard thereto. F. Barzegar and D. Y. Momodu acknowledge financial support from the University of Pretoria and the NRF for their PhD bursaries, while A. Bello acknowledges NRF through SARChI in Carbon Technology and Materials and University of Pretoria for his Postdoctoral financial support. A.T. C. Johnson acknowledges support from the Laboratory for Research on the Structure of Matter, National Science Foundation MRSEC, grant number DMR-1120901.

[1] P.J. Hall, M. Mirzaeian, S.I. Fletcher, F.B. Sillars, A.J.R. Rennie, G.O. Shitta-Bey, G. Wilson, A. Cruden, and R. Carter, Energy Environ. Sci. **3**, 1238 (2010).
[2] P. Simon, Y. Gogotsi, and B. Dunn, Science **343**, 1210 (2014).
[3] M. Inagaki, H. Konno, and O. Tanaike, J. Power Sources **195**, 7880 (2010).
[4] M.D. Stoller and R.S. Ruoff, Energy Environ. Sci. **3**, 1294 (2010).
[5] L. Zhang, F. Zhang, X. Yang, G. Long, Y. Wu, T. Zhang, K. Leng, Y. Huang, Y. Ma, A. Yu, and C. Yongsheng, Sci. Rep. **3** (2013).
[6] W.G. Pell and B.E. Conway, J. Power Sources **136**, 334 (2004).
[7] P. Hapiot and C. Lagrost, Chem. Rev. **108**, 2238 (2008).
[8] G.P. Pandey and A.C. Rastogi, J. Electrochem. Soc. **159**, A1664 (2012).
[9] H. Yu, J. Wu, L. Fan, K. Xu, X. Zhong, Y. Lin, and J. Lin, Electrochim. Acta **56**, 6881 (2011).
[10] C. Ramasamy, J. Palma del vel, and M. Anderson, J. Solid State Electrochem. **18**, 2217 (2014).
[11] P. Sivaraman, A. Thakur, R.K. Kushwaha, D. Ratna, and A.B. Samui, Electrochem. Solid-State Lett. **9**, A435 (2006).
[12] P. Yang, W. Cui, L. Li, L. Liu, and M. An, Solid State Sci. **14**, 598 (2012).

[13] M. Armand, F. Endres, D.R. MacFarlane, H. Ohno, and B. Scrosati, Nat. Mater. **8**, 621 (2009).
[14] P. Simon and Y. Gogotsi, Nat. Mater. **7**, 845 (2008).
[15] C.-C. Yang, S.-T. Hsu, and W.-C. Chien, J. Power Sources **152**, 303 (2005).
[16] C. Meng, C. Liu, L. Chen, C. Hu, and S. Fan, Nano Lett. **10**, 4025 (2010).
[17] S.A. Hashmi, R.J. Latham, R.G. Linford, and W.S. Schlindwein, Polym. Int. **47**, 28 (1998).
[18] G. Ma, E. Feng, K. Sun, H. Peng, J. Li, and Z. Lei, Electrochim. Acta **135**, 461 (2014).
[19] G. Ma, J. Li, K. Sun, H. Peng, J. Mu, and Z. Lei, J. Power Sources **256**, 281 (2014).
[20] H. Gao, F. Xiao, C.B. Ching, and H. Duan, ACS Appl. Mater. Interfaces **4**, 7020 (2012).
[21] A. Bello, K. Makgopa, M. Fabiane, D. Dodoo-Ahrin, K.I. Ozoemena, and N. Manyala, J. Mater. Sci. (2013).
[22] A. Bello, O.O. Fashedemi, J.N. Lekitima, M. Fabiane, D. Dodoo-Arhin, K.I. Ozoemena, Y. Gogotsi, A.T. Charlie Johnson, and N. Manyala, AIP Adv. **3**, 82118 (2013).
[23] L. Demarconnay, E. Raymundo-Pinero, and F. Béguin, Electrochem. Commun. **12**, 1275 (2010).
[24] J. Luo, H.D. Jang, and J. Huang, ACS Nano **7**, 1464 (2013).
[25] See supplementary material at http://dx.doi.org/10.1063/1.4931956 for comparison of galvanostatic charge/discharge at 0.5 A g-1 AC and CB electrode materials in PKC and PK gel electrolytes respectively and AC and PANI electrode materials in PKP and PK gel electrolytes respectively.